Acta Mech 221, 11–22 (2011)
DOI 10.1007/s00707-011-0485-z

Peng Li · Feng Jin · Zhenghua Qian

Propagation of thickness-twist waves in an inhomogeneous piezoelectric plate with an imperfectly bonded interface

Received: 7 October 2010 / Published online: 10 April 2011

Abstract The propagation of thickness-twist waves in an inhomogeneous piezoelectric plate with an imperfectly bonded interface is investigated. Based on the spring-type relation, the imperfectly bonded interface is dealt with, and the exact solution is obtained from the equations of the linear theory of piezoelectricity. The amplitude ratio between the incident wave and the reflected wave, the displacement component and the stress component are all obtained and plotted. Both theoretical analysis and numerical examples show that the effect of the mechanical imperfection on the wave propagation is more evident than that of the electrical imperfection. When the incident wave frequency and the mechanical imperfect parameter meet some particular relation, no reflected waves can appear in the piezoelectric plate. The results are of fundamental importance to the design of resonators and other devices when imperfect joints are considered.

1 Introduction

Waves in elastic and piezoelectric structures are widely used to make various acoustic wave devices including resonators for time-keeping and frequency control, sensors for information gathering and filters for telecommunication, etc. [1,2]. This includes both the so-called surface acoustic waves (SAW) and bulk acoustic waves (BAW). Thickness-twist vibration modes of crystal plates are often used as the operating modes for resonators and acoustic wave sensors [3–5]. When the sixfold axis of a 6 mm crystal is parallel to the major surface of a plate, thickness-twist waves can propagate in an unbounded plate [6]. The thickness-twist mode also exists in an inhomogeneous piezoelectric plate, such as the plate in which the central portion is different from the rest portions [7], the plate with a joint between two semi-infinite piezoelectric plates [8] and the plate which consists of multisectioned piezoelectric materials [9] etc.

Most of the work is on perfect bonding between the two layers [10–12]. It has been recently pointed out that imperfect bonding sometimes exists in devices, e.g., the aging of the glue which is applied at an interface, the defection of fabrication, and corrosion of the materials, [13,14]. Jin et al. [15] and Liu et al. [16] have investigated the effect of the imperfect interface on the propagation of Love waves in homogenous piezoelectric layered structures and graded composite structures, respectively. In the simplest description of the mechanical behavior of an imperfect interface, the interface can be treated as a layer that geometrically has a zero thickness but still possesses elasticity and interface elastic strain energy, e.g., the shear-lag model in which the tangential

P. Li · F. Jin (✉)
MOE Key Laboratory for Strength and Vibration, School of Aerospace,
Xi'an Jiaotong University, 710049 Xi'an, People's Republic of China
E-mail: jinfengzhao@263.net
Fax: +86-29-82665937

Z. Qian
Department of Mechanical and Environmental Informatics,
Tokyo Institute of Technology, Tokyo 152-8550, Japan

displacement at an interface is allowed to be different from both sides of the interface in order to account for the deformation of the interface layer [17,18].

In the present contribution, we investigate the effect of the imperfectly bonded interface in an inhomogeneous piezoelectric plate with a joint between two semi-infinite piezoelectric plates on the properties of thickness-twist waves by using a spring-type relation [19], which is different from the shear-lag model [17,18]. Different from the previous work [15–17], the mechanical imperfection and the electrical imperfection are all taken into account simultaneously. Since the material tensors of crystals of 6 mm symmetry have the same structures as polarized ceramics, our analysis is also valid for 6 mm piezoelectric crystals. This includes widely used materials like ZnO and AlN.

2 Governing equations and propagating wave solutions

Consider an inhomogeneous piezoelectric plate of uniform thickness $2h$, which consists of two different 6 mm crystals or polarized ceramics, as shown in Fig. 1. The ceramic material is poled in the x_3 direction determined by the right-hand rule from the x_1 and x_2 axes. The left portion $x_1 < 0$ is made of one piezoelectric material, and the right portion $x_1 > 0$ is made of another one. The interface of the two materials $x_1 = 0$ is assumed to be imperfect. The plate is unelectroded, and the surfaces are traction free at $x_2 = \pm h$.

2.1 Governing equations

Due to the relatively high symmetry of 6 mm crystals, the structure allows simple and exact modes with only one anti-plane displacement u_3, which is coupled with the electric potential φ i.e., thickness-twist waves [7–9]

$$u_1 = 0, u_2 = 0, u_3 = u(x_1, x_2, t), \quad \varphi = \varphi(x_1, x_2, t) \tag{1}$$

which are governed by

$$c\nabla^2 u + e\nabla^2\varphi = \rho\ddot{u}, \quad e\nabla^2 u - \varepsilon\nabla^2\varphi = 0 \tag{2}$$

where the elastic constant, the piezoelectric, and the dielectric permittivity coefficients are $c = c_{44}$, $e = e_{15}$, and $\varepsilon = \varepsilon_{11}$, respectively. The dot denotes time differentiation, and ρ is the mass density. A function ψ can be introduced through $\varphi = \psi + eu/\varepsilon$ [8–10], and the governing equations for u and ψ are

$$\bar{c}\nabla^2 u = \rho\ddot{u}, \quad \nabla^2\psi = 0 \tag{3}$$

in which $\nabla^2 = \partial^2/\partial x_1^2 + \partial^2/\partial x_2^2$ is the Laplace Operator, and $\bar{c} = c + e^2/\varepsilon$. The nontrivial stress and the electric displacement components are

$$\begin{aligned} T_{32} &= \bar{c}u_{,2} + e\psi_{,2}, \quad T_{31} = \bar{c}u_{,1} + e\psi_{,1} \\ D_2 &= -\varepsilon\psi_{,2}, \quad D_1 = -\varepsilon\psi_{,1} \end{aligned} \tag{4}$$

where an index after a comma denotes partial differentiation with respect to the relative coordinate.

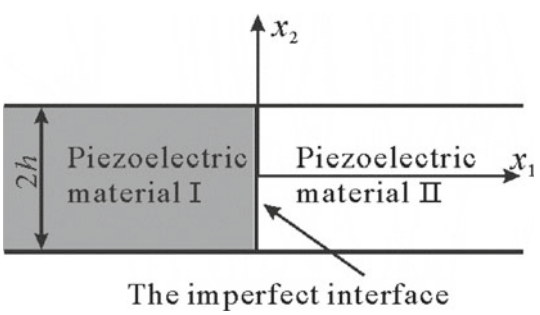

Fig. 1 An inhomogeneous piezoelectric plate with an imperfectly bonded interface

2.2 Boundary conditions

For the unelectroded and traction-free surfaces, $D_2 = 0$ and $T_{23} = 0$ at $x_2 = \pm h$, this is equal to

$$x_2 = \pm h : u_{,2} = 0, \quad \psi_{,2} = 0. \tag{5}$$

For the imperfectly bonded interface at $x_1 = 0$, we adopt the spring-type relation [19], which requires

$$x_1 = 0 : \begin{cases} T_{13}^{+} = T_{13}^{-} = K(u^{+} - u^{-}) \\ D_1^{+} = D_1^{-} = \Gamma(\varphi^{+} - \varphi^{-}) \end{cases} \tag{6}$$

where $K(\mathrm{N/m^3})$ is the effective interface elastic stiffness parameter, and $\Gamma(\mathrm{C/Vm^2})$ is the electrical imperfection parameter, which simultaneously describe how well the two materials are bonded. When $K = 0$ and $\Gamma = 0$, the two half-spaces lose their mechanical and electrical interaction. When $K = \infty$ and $\Gamma \neq \infty$, we consider the electrical imperfection only. The circumstance of $\Gamma = \infty$ and $K \neq \infty$ is the only consideration of the mechanical imperfection, which is the same as the shear-lag model [15–18]. The case of $K = \infty$ and $\Gamma = \infty$ is for the perfect interface with continuous displacement and electric function across the joint.

2.3 An exact propagating wave solution

Assume that an incident wave comes from $x_1 = -\infty$, travels normally at the imperfect interface $x_1 = 0$, reflects, and transmits. Following Yang et al. [7], the solutions to Eq. (3) can be classified into waves symmetric or anti-symmetric in x_2. Taking the symmetric modes for example, u and ψ can be written as

$$x_1 \leq 0 : \begin{cases} u = \cos(\xi_2 x_2)[A_1 \exp(i\xi_1 x_1) + A_2 \exp(-i\xi_1 x_1)] \exp(-i\omega t) \\ \psi = \cos(\xi_2 x_2) B \exp(\xi_2 x_1) \exp(-i\omega t) \end{cases} \tag{7.1}$$

$$x_1 \geq 0 : \begin{cases} u = \cos(\xi_2 x_2) A' \exp\left[i\left(\xi_1' x_1 - \omega t\right)\right] \\ \psi = \cos(\xi_2 x_2) B' \exp(-\xi_2 x_1) \exp(-i\omega t) \end{cases} \tag{7.2}$$

where A_1, A_2, and A' stand for the incident wave, the reflected wave, and the transmitted wave, respectively; B and B' represent a nonpropagating field localized near the joint. ω is the wave frequency, and $i^2 = -1$. Considering Eqs. (3) and (5), ξ_2, ξ_1, and ξ_1' satisfy

$$\begin{aligned} \xi_2 &= \frac{m\pi}{2h}, \quad m = 0, 2, 4, \ldots, \\ \xi_1 &= \sqrt{\frac{\rho\omega^2}{\bar{c}} - \xi_2^2} = \sqrt{\frac{\rho}{\bar{c}}}\sqrt{\omega^2 - \left(\frac{m\pi}{2h}\right)^2 \frac{\bar{c}}{\rho}} = \frac{1}{v_T}\sqrt{\omega^2 - \omega_{\mathrm{m}}^2}, \\ \xi'_1 &= \sqrt{\frac{\rho'\omega^2}{\bar{c}'} - \xi_2^2} = \sqrt{\frac{\rho'}{\bar{c}'}}\sqrt{\omega^2 - \left(\frac{m\pi}{2h}\right)^2 \frac{\bar{c}'}{\rho'}} = \frac{1}{v_T'}\sqrt{\omega^2 - \omega_{\mathrm{m}}'^2} \end{aligned} \tag{8}$$

where $v_T = \sqrt{\bar{c}/\rho}$ and $v_T' = \sqrt{\bar{c}'/\rho'}$ are the bulk shear wave velocities of the piezoelectric material occupying $x_1 < 0$ and $x_1 > 0$, respectively. $\omega_{\mathrm{m}}^2 = (\frac{m\pi}{2h})^2 \frac{\bar{c}}{\rho}$ and $\omega_{\mathrm{m}}'^2 = (\frac{m\pi}{2h})^2 \frac{\bar{c}'}{\rho'}$ are the cutoff frequencies of thickness-twist waves in the left and right portions. In particular, $m = 0$ is called the face-shear mode, which will not be considered here [7].

Equation (7) has already satisfied Eqs. (3) and (5), so inserting Eq. (7) into (4), we can get

$$x_1 \leq 0 : \begin{cases} T_{31} = \cos(\xi_2 x_2)\{i\xi_1 \bar{c}[A_1 \exp(i\xi_1 x_1) - A_2 \exp(-i\xi_1 x_1)] + e\xi_2 B \exp(\xi_2 x_1)\} \exp(-i\omega t), \\ D_1 = \cos(\xi_2 x_2)[-\varepsilon\xi_2 B \exp(\xi_2 x_1)] \exp(i\omega t), \end{cases} \tag{9.1}$$

$$x_1 \geq 0 : \begin{cases} T_{31} = \cos(\xi_2 x_2)\left[i\xi_1' \bar{c}' A' \exp\left(i\xi_1' x_1\right) - e'\xi_2 B' \exp(-\xi_2 x_1)\right] \exp(-i\omega t), \\ D_1 = \cos(\xi_2 x_2)[\varepsilon'\xi_2 B' \exp(-\xi_2 x_1)] \exp(i\omega t). \end{cases} \tag{9.2}$$

Substituting Eq. (9) into (6) gives

$$\begin{aligned}
&i\xi_1'\bar{c}'A' - e'\xi_2 B' = i\xi_1\bar{c}A_1 - i\xi_1\bar{c}A_2 + e\xi_2 B,\\
&i\xi_1'\bar{c}'A' - e'\xi_2 B' = K(A' - A_1 - A_2),\\
&-\varepsilon\xi_2 B = \varepsilon'\xi_2 B',\\
&\varepsilon'\xi_2 B' = \Gamma\left(B' + \frac{e'}{\varepsilon'}A' - B - \frac{e}{\varepsilon}A_1 - \frac{e}{\varepsilon}A_2\right).
\end{aligned} \tag{10}$$

We rewrite the above equations into the following form:

$$\begin{bmatrix}
i\xi_1\bar{c} & -e\xi_2 & i\xi_1'\bar{c}' & -e'\xi_2\\
1 & 0 & -1 + \frac{i\xi_1'\bar{c}'}{K} & \frac{-e'\xi_2}{K}\\
0 & \varepsilon & 0 & \varepsilon'\\
\frac{e}{\varepsilon} & 1 & -\frac{e'}{\varepsilon'} & -1 + \frac{\varepsilon'\xi_2}{\Gamma}
\end{bmatrix}
\begin{Bmatrix} A_2\\ B\\ \mathrm{A}'\\ B' \end{Bmatrix}
= \begin{Bmatrix} i\xi_1\bar{c}\\ -1\\ 0\\ -\frac{e}{\varepsilon} \end{Bmatrix} A_1. \tag{11}$$

According to Eq. (11), we can obtain the ratio A_2/A_1, A'/A_1, B/A_1 and B'/A_1

$$\frac{A_2}{A_1} = \frac{\Delta_1}{\Delta}, \quad \frac{A'}{A_1} = \frac{\Delta_2}{\Delta}, \quad \frac{B}{A_1} = \frac{\Delta_3}{\Delta}, \quad \frac{B'}{A_1} = \frac{\Delta_4}{\Delta} \tag{12}$$

where

$$\begin{aligned}
\Delta &= -\left(i\xi_1\bar{c} + i\xi_1'\bar{c}'\right)(\varepsilon + \varepsilon') - \varepsilon\varepsilon'\xi_2\left(\frac{e}{\varepsilon} - \frac{e'}{\varepsilon'}\right)^2 + \frac{\varepsilon\varepsilon'\xi_2}{\Gamma}\left(i\xi_1\bar{c} + i\xi_1'\bar{c}'\right) + \frac{\xi_1\bar{c}\xi_1'\bar{c}'\varepsilon\varepsilon'\xi_2}{K\Gamma}\\
&\quad + \frac{1}{K}\left\{-\xi_1\bar{c}\xi_1'\bar{c}'(\varepsilon + \varepsilon') + \varepsilon\varepsilon'\xi_2\left[i\xi_1'\bar{c}'\left(\frac{e}{\varepsilon}\right)^2 + i\xi_1\bar{c}\left(\frac{e'}{\varepsilon'}\right)^2\right]\right\},\\
\Delta_1 &= (\varepsilon + \varepsilon')\left(i\xi_1'\bar{c}' - i\xi_1\bar{c}\right) + \varepsilon\varepsilon'\xi_2\left(\frac{e}{\varepsilon} - \frac{e'}{\varepsilon'}\right)^2 + \frac{\varepsilon\varepsilon'\xi_2}{\Gamma}\left(i\xi_1\bar{c} - i\xi_1'\bar{c}'\right) + \frac{\xi_1\bar{c}\xi_1'\bar{c}'\varepsilon\varepsilon'\xi_2}{K\Gamma}\\
&\quad + \frac{1}{K}\left\{-\xi_1\bar{c}\xi_1'\bar{c}'(\varepsilon + \varepsilon') + \varepsilon\varepsilon'\xi_2\left[i\xi_1\bar{c}\left(\frac{e'}{\varepsilon'}\right)^2 - i\xi_1'\bar{c}'\left(\frac{e}{\varepsilon}\right)^2\right]\right\},\\
\Delta_2 &= -2i\xi_1\bar{c}(\varepsilon + \varepsilon') + 2i\xi_1\bar{c}\xi_2\left(\frac{ee'}{K} + \frac{\varepsilon\varepsilon'}{\Gamma}\right), \Delta_3 = 2i\xi_1\bar{c}\varepsilon'\left(\frac{e}{\varepsilon} - \frac{e'}{\varepsilon'}\right) + \frac{1}{K}2\xi_1\bar{c}\xi_1'\bar{c}'e\frac{\varepsilon'}{\varepsilon},\\
\Delta_4 &= 2i\xi_1\bar{c}\varepsilon\left(\frac{e}{\varepsilon} - \frac{e'}{\varepsilon'}\right) - \frac{1}{K}2\xi_1\bar{c}\xi_1'\bar{c}'e.
\end{aligned} \tag{13}$$

2.4 Some observation on the imperfect joint

We examine below some special cases of the two parameters K and Γ, which are used to define the imperfect joint.

(A) If we only consider the mechanical imperfection, i.e., $K \neq 0$ and $\Gamma = \infty$, which is the same as a shear-lag model, Eq. (13) can be written as

$$\begin{aligned}
\Delta &= -\left(i\xi_1\bar{c} + i\xi_1'\bar{c}'\right)(\varepsilon+\varepsilon') - \varepsilon\varepsilon'\xi_2\left(\frac{e}{\varepsilon} - \frac{e'}{\varepsilon'}\right)^2 \\
&\quad + \frac{1}{K}\left\{-\xi_1\bar{c}\xi_1'\bar{c}'(\varepsilon+\varepsilon') + \varepsilon\varepsilon'\xi_2\left[i\xi_1'\bar{c}'\left(\frac{e}{\varepsilon}\right)^2 + i\xi_1\bar{c}\left(\frac{e'}{\varepsilon'}\right)^2\right]\right\}, \\
\Delta_1 &= (\varepsilon+\varepsilon')\left(i\xi_1'\bar{c}' - i\xi_1\bar{c}\right) + \varepsilon\varepsilon'\xi_2\left(\frac{e}{\varepsilon} - \frac{e'}{\varepsilon'}\right)^2 \\
&\quad + \frac{1}{K}\left\{-\xi_1\bar{c}\xi_1'\bar{c}'(\varepsilon+\varepsilon') + \varepsilon\varepsilon'\xi_2\left[i\xi_1\bar{c}\left(\frac{e'}{\varepsilon'}\right)^2 - i\xi_1'\bar{c}'\left(\frac{e}{\varepsilon}\right)^2\right]\right\}, \\
\Delta_2 &= -2i\xi_1\bar{c}(\varepsilon+\varepsilon') + 2i\xi_1\bar{c}\xi_2\frac{ee'}{K}, \quad \Delta_3 = 2i\xi_1\bar{c}\varepsilon'\left(\frac{e}{\varepsilon} - \frac{e'}{\varepsilon'}\right) + \frac{1}{K}2\xi_1\bar{c}\xi_1'\bar{c}'e\frac{\varepsilon'}{\varepsilon}, \\
\Delta_4 &= 2i\xi_1\bar{c}\varepsilon\left(\frac{e}{\varepsilon} - \frac{e'}{\varepsilon'}\right) - \frac{1}{K}2\xi_1\bar{c}\xi_1'\bar{c}'e.
\end{aligned} \tag{14}$$

(B) Similarly, if we consider the electrical imperfection only, i.e., $\Gamma \neq 0$ and $K = \infty$, Eq. (13) can be written as

$$\begin{aligned}
\Delta &= -\left(i\xi_1\bar{c} + i\xi_1'\bar{c}'\right)(\varepsilon+\varepsilon') - \varepsilon\varepsilon'\xi_2\left(\frac{e}{\varepsilon} - \frac{e'}{\varepsilon'}\right)^2 + \frac{\varepsilon\varepsilon'\xi_2}{\Gamma}\left(i\xi_1\bar{c} + i\xi_1'\bar{c}'\right), \\
\Delta_1 &= (\varepsilon+\varepsilon')\left(i\xi_1'\bar{c}' - i\xi_1\bar{c}\right) + \varepsilon\varepsilon'\xi_2\left(\frac{e}{\varepsilon} - \frac{e'}{\varepsilon'}\right)^2 + \frac{\varepsilon\varepsilon'\xi_2}{\Gamma}\left(i\xi_1\bar{c} - i\xi_1'\bar{c}'\right), \\
\Delta_2 &= -2i\xi_1\bar{c}(\varepsilon+\varepsilon') + 2i\xi_1\bar{c}\xi_2\frac{\varepsilon\varepsilon'}{\Gamma}, \ \Delta_3 = 2i\xi_1\bar{c}\varepsilon'\left(\frac{e}{\varepsilon} - \frac{e'}{\varepsilon'}\right), \ \Delta_4 = 2i\xi_1\bar{c}\varepsilon\left(\frac{e}{\varepsilon} - \frac{e'}{\varepsilon'}\right).
\end{aligned} \tag{15}$$

(C) If the interface is perfect, i.e., $K = \infty$ and $\Gamma = \infty$ simultaneously, Eq. (13) can be written as

$$\begin{aligned}
&\Delta = -\left(i\xi_1\bar{c} + i\xi_1'\bar{c}'\right)(\varepsilon+\varepsilon') - \varepsilon\varepsilon'\xi_2\left(\frac{e}{\varepsilon} - \frac{e'}{\varepsilon'}\right)^2, \ \Delta_1 = (\varepsilon+\varepsilon')\left(i\xi_1'\bar{c}' - i\xi_1\bar{c}\right) + \varepsilon\varepsilon'\xi_2\left(\frac{e}{\varepsilon} - \frac{e'}{\varepsilon'}\right)^2, \\
&\Delta_2 = -2i\xi_1\bar{c}(\varepsilon+\varepsilon'), \ \Delta_3 = 2i\xi_1\bar{c}\varepsilon'\left(\frac{e}{\varepsilon} - \frac{e'}{\varepsilon'}\right), \ \Delta_4 = 2i\xi_1\bar{c}\varepsilon\left(\frac{e}{\varepsilon} - \frac{e'}{\varepsilon'}\right)
\end{aligned} \tag{16}$$

which possesses exactly the same expressions as obtained in the work by Yang [8].

(D) When $K = 0$ and $\Gamma = 0$, the two piezoelectric materials lose completely both their mechanical and electrical interaction.

A detailed comparison between Eqs. (14) and (15) is listed in Table 1, which could theoretically give us an illustration on how much different the two imperfections affect the field quantities when the thickness-twist waves propagate through the imperfect joint. Some simple discussion can be made below.

Table 1 The contrasting between the mechanical imperfection and the electrical imperfection

	The mechanical imperfection	The electrical imperfection
Δ	$\frac{1}{K}\left\{-\xi_1\bar{c}\xi_1'\bar{c}'(\varepsilon+\varepsilon') + \varepsilon\varepsilon'\xi_2\left[i\xi_1'\bar{c}'\left(\frac{e}{\varepsilon}\right)^2 + i\xi_1\bar{c}\left(\frac{e'}{\varepsilon'}\right)^2\right]\right\}$	$\frac{\varepsilon\varepsilon'\xi_2}{\Gamma}\left(i\xi_1\bar{c} + i\xi_1'\bar{c}'\right)$
Δ_1	$\frac{1}{K}\left\{-\xi_1\bar{c}\xi_1'\bar{c}'(\varepsilon+\varepsilon') + \varepsilon\varepsilon'\xi_2\left[i\xi_1\bar{c}\left(\frac{e'}{\varepsilon'}\right)^2 - i\xi_1'\bar{c}'\left(\frac{e}{\varepsilon}\right)^2\right]\right\}$	$\frac{\varepsilon\varepsilon'\xi_2}{\Gamma}\left(i\xi_1\bar{c} - i\xi_1'\bar{c}'\right)$
Δ_2	$2i\xi_1\bar{c}\xi_2\frac{ee'}{K}$	$2i\xi_1\bar{c}\xi_2\frac{\varepsilon\varepsilon'}{\Gamma}$
Δ_3	$\frac{1}{K}2\xi_1\bar{c}\xi_1'\bar{c}'e\frac{\varepsilon'}{\varepsilon}$	0
Δ_4	$-\frac{1}{K}2\xi_1\bar{c}\xi_1'\bar{c}'e$	0

For Δ, the dominant term $-\xi_1\bar{c}\xi_1'\bar{c}'(\varepsilon+\varepsilon')/K$ for the mechanical imperfection has the order of the product of $\bar{c}$ and $\bar{c}'$, while the term $\varepsilon\varepsilon'\xi_2(i\xi_1\bar{c}+i\xi_1'\bar{c}')/\Gamma$ for the electrical imperfection has the order of the summation of $\bar{c}$ and $\bar{c}'$. Generally speaking, $\bar{c}$ and $\bar{c}'$ have the order of 10^{10}. Hence, when K and Γ take the same value simultaneously, the effect of the mechanical imperfection is much larger than that of the electrical imperfection. For Δ_1, we can get the same conclusion.
For Δ_2, the ratio of the term $2i\xi_1\bar{c}\xi_2 ee'/K$ for the mechanical imperfection to the term $2i\xi_1\bar{c}\xi_2\varepsilon\varepsilon'/\Gamma$ for the electrical imperfection is $\frac{(ee'/K)}{(\varepsilon\varepsilon'/\Gamma)}$. Obviously, the effect of the mechanical imperfection is more evident than that of the electrical imperfection when K and Γ have the same value simultaneously. For Δ_3 and Δ_4, the same conclusion can be obtained easily.

3 Numerical examples

As we know, the plate cannot propagate the waves single with the frequency which is smaller than the cutoff frequency of the left portion [20,21], so the frequency of the incident wave satisfies $\omega > \omega_{\mathrm{m}}$. We choose PZT5 and PZT6B for the left and right portions, respectively. The corresponding material parameters are listed in Table 2 [22]. As a numerical example we consider the case $m = 2$, and the plate thickness is chosen to be $h = 1$ mm.

3.1 The contrast between the mechanical imperfection and the electrical imperfection

In the previous Sections, we have concluded that the effect of the mechanical imperfection is more evident than that of the electrical imperfection. In order to prove the above conclusion further, we calculate A_2/A_1 and A'/A_1 by using the same selected values for K and Γ when one of them is fixed to infinity. The results are listed in Table 3.

It can be seen from Table 3 that the electrical imperfection basically has no effect on the values of A_2/A_1 and A'/A_1, while the mechanical imperfection has a significant effect on the values of A_2/A_1 and A'/A_1, which are consistent with the conclusion obtained from previous theoretical analysis. In the following discussion, we will ignore the electrical imperfection and consider the mechanical imperfection only, i.e., $\Gamma = \infty$ and $K \neq \infty$. Furthermore, when the interface is perfect ($K = \infty, \Gamma = \infty$), the displacement component is continuous, i.e., $A_2/A_1 + 1 = A'/A_1$. On the other hand, the displacement component is not continuous for

Table 2 The material parameters used in the numerical computation

Materials	ρ (kg/m^3)	c (10^{10} N/m^2)	e (C/m^2)	ε (10^{-8} C/Vm)
PZT-6B	7550	3.55	4.6	0.360
PZT-5	7750	2.11	12.3	0.811

Table 3 A_2/A_1 and A'/A_1 at the same value of K and Γ

ω		K and Γ	A_2/A_1	A'/A_1
$\omega = 7.235$ MHz	$\Gamma = \infty$	$K = \infty$	0.00445413	1.00445413
	$\Gamma = \infty$	$K = 1.0 \times 10^{16}$ N/m^3	0.00734808	1.00475790
		$K = 0.5 \times 10^{16}$ N/m^3	0.01024418	1.00505441
		$K = 0.2 \times 10^{16}$ N/m^3	0.01894504	1.00590011
	$K = \infty$	$\Gamma = 1.0 \times 10^{16}$ C/Vm^2	0.00445413	1.00445413
		$\Gamma = 0.5 \times 10^{16}$ C/Vm^2	0.00445413	1.00445413
		$\Gamma = 0.2 \times 10^{16}$ C/Vm^2	0.00445413	1.00445413
$\omega = 7.474$ MHz	$\Gamma = \infty$	$K = \infty$	0.26123128	1.26123128
	$\Gamma = \infty$	$K = 1.0 \times 10^{15}$ N/m^3	0.30975491	1.21421480
		$K = 0.8 \times 10^{15}$ N/m^3	0.33170382	1.18645000
		$K = 0.5 \times 10^{15}$ N/m^3	0.42774050	1.05035898
	$K = \infty$	$\Gamma = 1.0 \times 10^{15}$ C/Vm^2	0.26123128	1.26123128
		$\Gamma = 0.8 \times 10^{15}$ C/Vm^2	0.26123128	1.26123128
		$\Gamma = 0.5 \times 10^{15}$ C/Vm^2	0.26123128	1.26123128

the imperfect interface ($K \neq \infty$) i.e., $A_2/A_1 + 1 \neq A'/A_1$. This point can be clearly seen from Table 3, which validates the correctness of our numerical calculation.

3.2 The effect of imperfection when the frequency of the incident wave ω satisfies $\omega_m < \omega < \omega'_m$

Figures 2a, b show, respectively, the amplitude ratio between the incident wave and the reflected wave A_2/A_1 as the function with the frequency of the incident wave ω and the effective interface elastic stiffness K at the interface $x_1 = 0$. If the interface approaches perfectly, i.e., $K = \infty$, the relation between A_2/A_1 and ω is linear, which can be seen from Fig. 2a clearly. Meanwhile, if the interface is imperfect, i.e., $K \neq \infty$, this sort of relationship becomes nonlinear, and with the increasing of the imperfection the tendency of the nonlinearity becomes more and more evident. It can be concluded from Fig. 2a, b that the imperfect bonding makes the reflected wave stronger (i.e., A_2/A_1 becomes larger) when the incident wave frequency ω keeps constant, while the larger the incident wave frequency is, the stronger the reflected wave becomes as K keeps constant.

Especially, considering the perfect interface, the value of A_2/A_1 is zero when the frequency takes some value between 7.23 MHz and 7.24 MHz. In other words, the incident wave with such a critical frequency will totally transmit across the joint, and at the same time, no waves will be reflected at the interface. With the

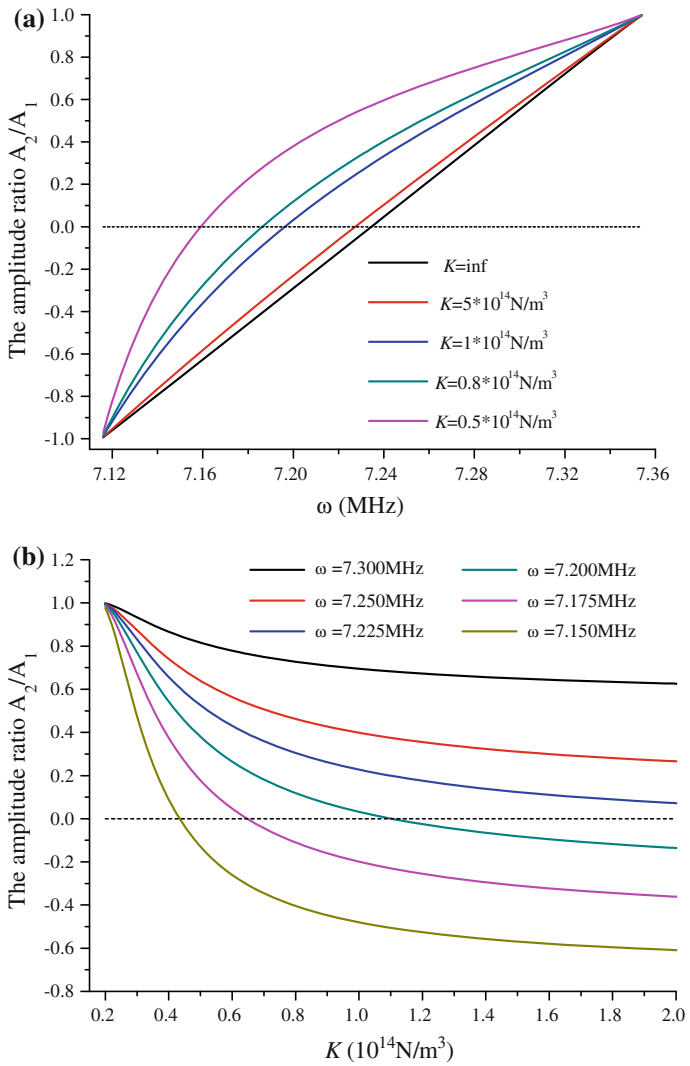

Fig. 2 The amplitude ratio between the incident wave and the reflected wave A_2/A_1 when the frequency of the incident wave ω follow $\omega_m < \omega < \omega'_m$. **a** A_2/A_1 as a function with the frequency of the incident wave ω; **b** A_2/A_1 as a function with the effective interface elastic stiffness K

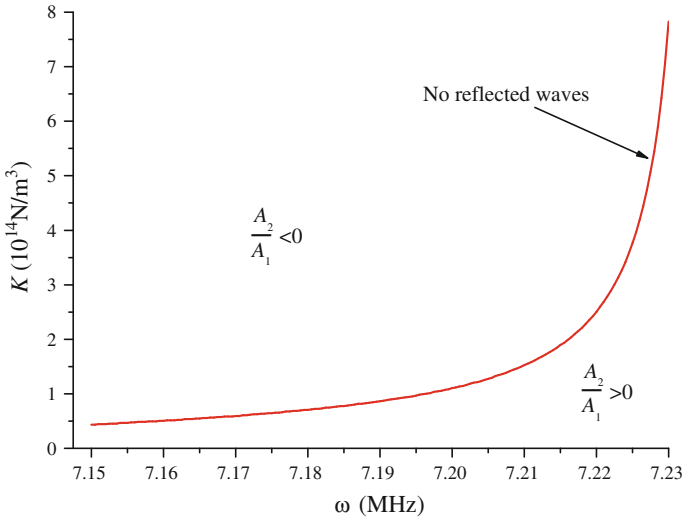

Fig. 3 The effective interface elastic stiffness K as a function with the critical frequency ω for zero-reflection

appearance of the imperfect bonding (i.e., K decreases from ∞), the critical frequency for zero-reflection becomes smaller. The relation between the critical frequency for zero-reflection and the imperfection K is depicted in Fig. 3.

When the imperfection K and the frequency of the incident wave ω follow the curve which is depicted as Fig. 3, some energy of the incident wave is assimilated, and the other transmits totally. No reflected waves can be received in the region $x_1 < 0$. Besides, above the curve $A_2/A_1 < 0$, which means the reflected wave makes the displacement of the incident wave weaker. Similarly, in the region below the curve, the reflected waves get stronger.

Figure 4 shows the relative displacement along the x_1 direction at the middle plane $x_2 = 0$ of the plate. The black curve is related to the perfect interface when $\omega = 7.235$ MHz that is the same as the results reported in reference [8], which also provides that our computation results are correct. The red line in Fig. 4 corresponds to the case of imperfect bonding and resembles the black line closely except for the displacement discontinuity at the imperfect joint, which is due to the spring-type relation we have adopted. Whether the interface is imperfect or not, the transmitted wave decays rapidly along the x_1 direction when the frequency satisfies $\omega_{\mathrm{m}} < \omega < \omega'_{\mathrm{m}}$. In the region $x_1 > 0.01$ m, the displacement almost equals zero, which means we cannot receive the transmitted waves in this region. This is related to the energy-trapping phenomenon of the thickness-twist modes [7–9]. For any point located in $0 < x_1 < 0.01$ m, the displacement in the case of imperfect bonding is a little bit smaller than that in the case of perfect bonding because the imperfect bonding also absorbs some energy of the waves when they propagate through it.

Defining $\delta T_{13} = \bar{T}_{13} - T^0_{13}$, in which T^0_{13} is the stress when the interface is perfect and $\bar{T}_{13}$ is the stress with the imperfect interface. Assuming $A_1 = 1 \times 10^{-4}\, m$, the stress T_{13} and the stress change δT_{13} can be calculated, results from which are shown in Fig. 5a, b, respectively. It can be seen from Fig. 5 that the distribution of T_{13} resembles that of the displacement distribution shown in Fig. 4, i.e., they fluctuate harmonically in the incident half but decay rapidly and monotonically to zero in the transmission half, which is also because of the energy-trapping phenomenon. However, different from Fig. 4, the stress T_{13} is continuous which is due to the spring-type relation we have adopted. On the other hand, it can be readily seen from Fig. 5b that with the increase of the imperfection (K decreases from ∞), the amplitude of δT_{13} in the incident half is gradually increased while the stress change in the transmission half is negligible except for the close vicinity of the joint. That means the imperfect bonding has more effect on the thickness-twist wave field in the incident half $x_1 < 0$ than that in the transmission half $x_1 > 0$ when $\omega_{\mathrm{m}} < \omega < \omega'_{\mathrm{m}}$, which is also due to the energy-trapping feature of the thickness-twist mode.

3.3 The effect of imperfection when the frequency of the incident wave ω satisfies $\omega > \omega'_{\mathrm{m}}$

Figures 6a, b show, respectively, the amplitude ratio between the incident wave and the reflected wave A_2/A_1 as the function with the frequency of the incident wave ω and the effective interface elastic stiffness K at the

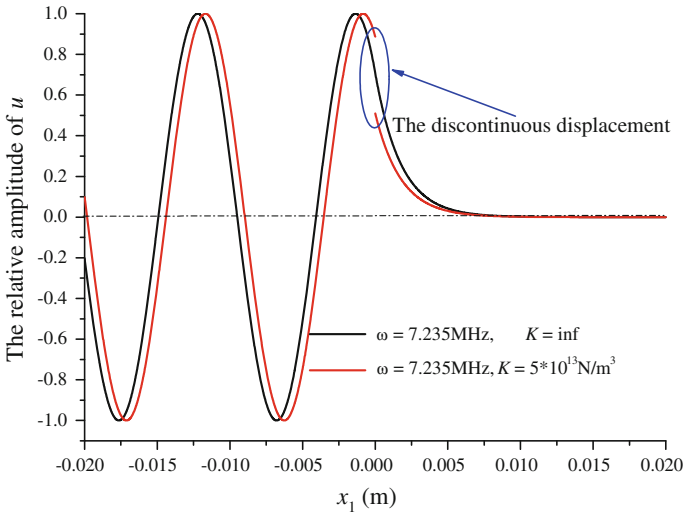

Fig. 4 The relative displacement when $\omega = 7.235\,\text{MHz}$

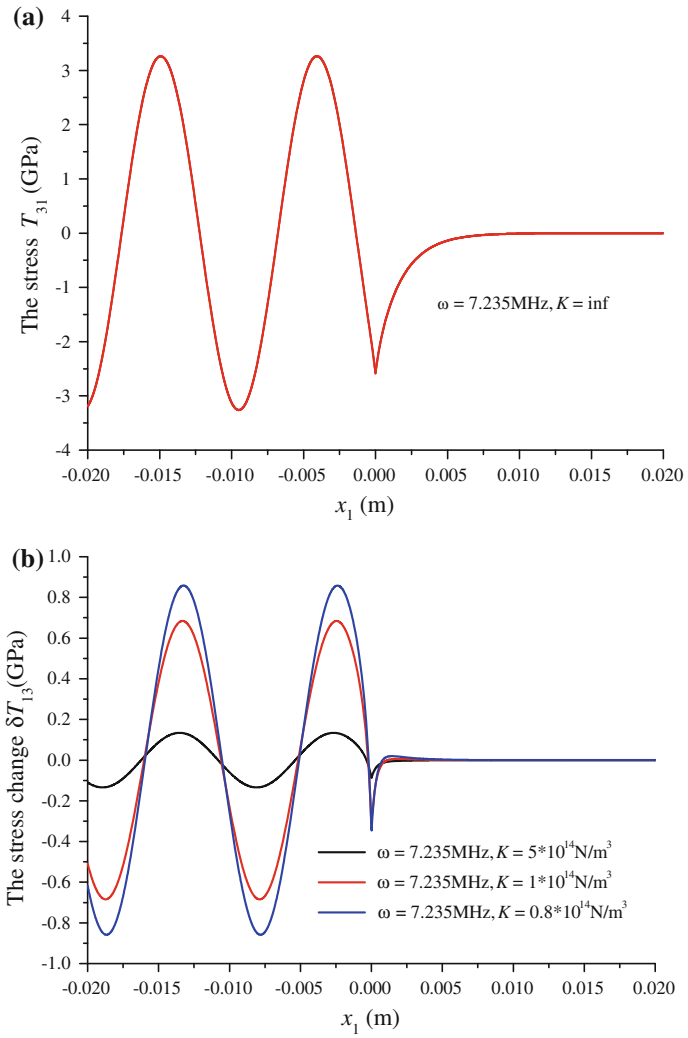

Fig. 5 The stress T_{13} and the stress change δT_{13} when $\omega = 7.235\,\text{MHz}$. **a** The stress T_{13}, **b** the stress change δT_{13}

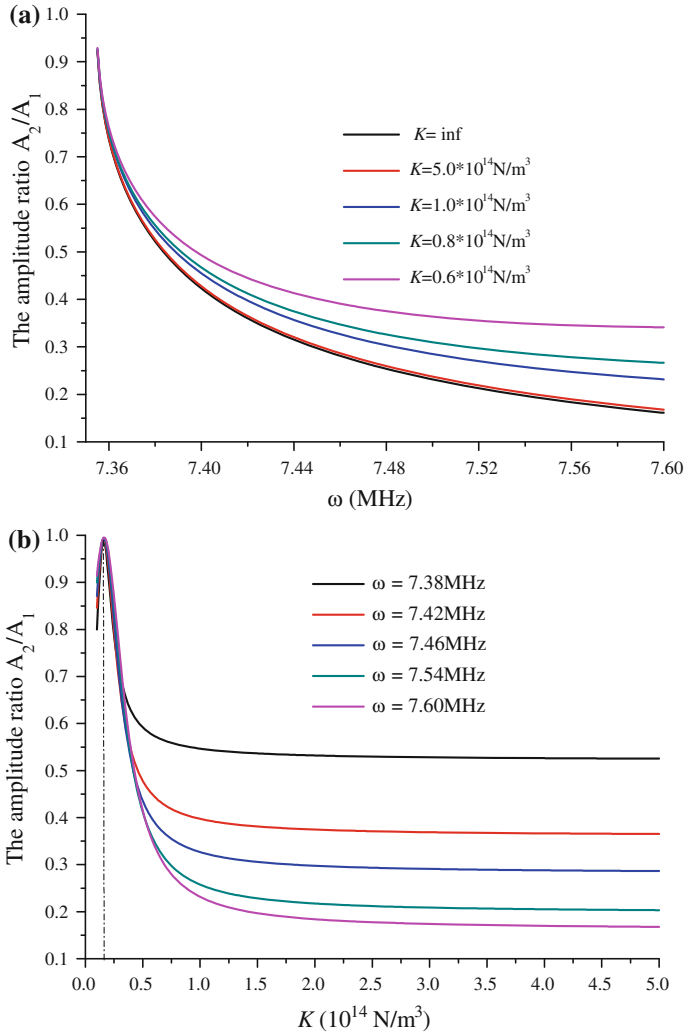

Fig. 6 The amplitude ratio between the incident wave and the reflected wave A_2/A_1 when the frequency of the incident wave ω satisfies $\omega > \omega_m'$. **a** A_2/A_1 as a function with the frequency of the incident wave ω; **b** A_2/A_1 as a function with the effective interface elastic stiffness K

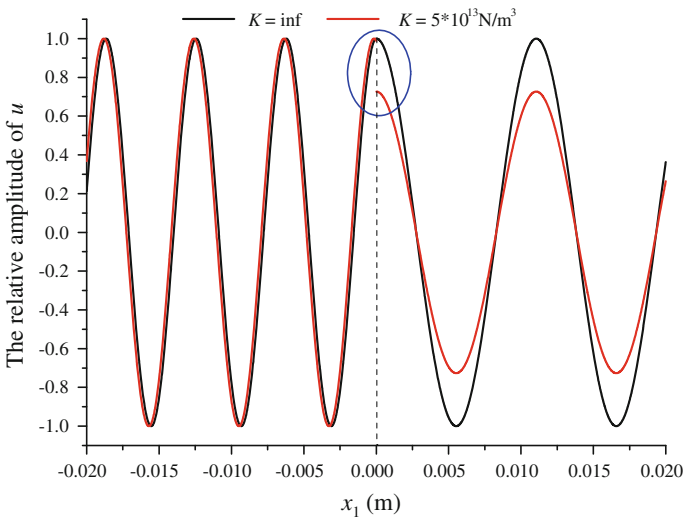

Fig. 7 The relative displacement when $\omega = 7.47$ MHz

joint $x_1 = 0$ when the frequency of the incident wave ω satisfies $\omega > \omega'_{\mathrm{m}}$. It can be seen readily that the amplitude ratio is never equal to zero, i.e., the incident wave does not achieve zero-reflection when the wave frequency satisfies $\omega > \omega'_{\mathrm{m}}$, which is different from the circumstance of $\omega_{\mathrm{m}} < \omega < \omega'_{\mathrm{m}}$. From Fig. 6a, we can conclude that the reflected waves get weaker and weaker with the increasing frequencies when K keeps unchanged. However, the effect of the imperfection is not monotonous when the frequency ω keeps constant, which can be seen from Fig. 6b. The reflected waves get stronger firstly, achieve the maximum value at about $K = 0.2 \times 10^{14}\ \mathrm{N/m^3}$, and then decrease, finally approach a steady value. The value of the imperfect parameter K at which the reflected waves take their maximum values is independent of the incident wave frequency.

Figure 7 shows the relative displacement along the x_1 direction at the middle plane $x_2 = 0$ of the plate when the frequency of the incident wave $\omega = 7.47\,\mathrm{MHz}$. The incident wave and the transmitted wave are all harmonic along the x_1 direction when the frequency satisfies $\omega > \omega'_{\mathrm{m}}$, which means there is no energy-trapping phenomenon. The red line in Fig. 7 corresponds to the case of imperfect bonding and resembles the black line closely except for the displacement discontinuity at the imperfect joint, which is similar to Fig. 4. It can also be seen that the imperfect joint absorbs some energy of the incident wave since the amplitude of the transmitted wave becomes smaller than that of the incident wave.

Figure 8 shows the stress and the stress change distribution along the x_1 direction at the middle plane $x_2 = 0$ of the plate when the frequency $\omega = 7.47\,\mathrm{MHz}$. The imperfection interface has a significant effect on the stress distribution when the frequency satisfies $\omega > \omega'_{\mathrm{m}}$. Especially, the effect of stress is most evident at the imperfect interface $x_1 = 0$.

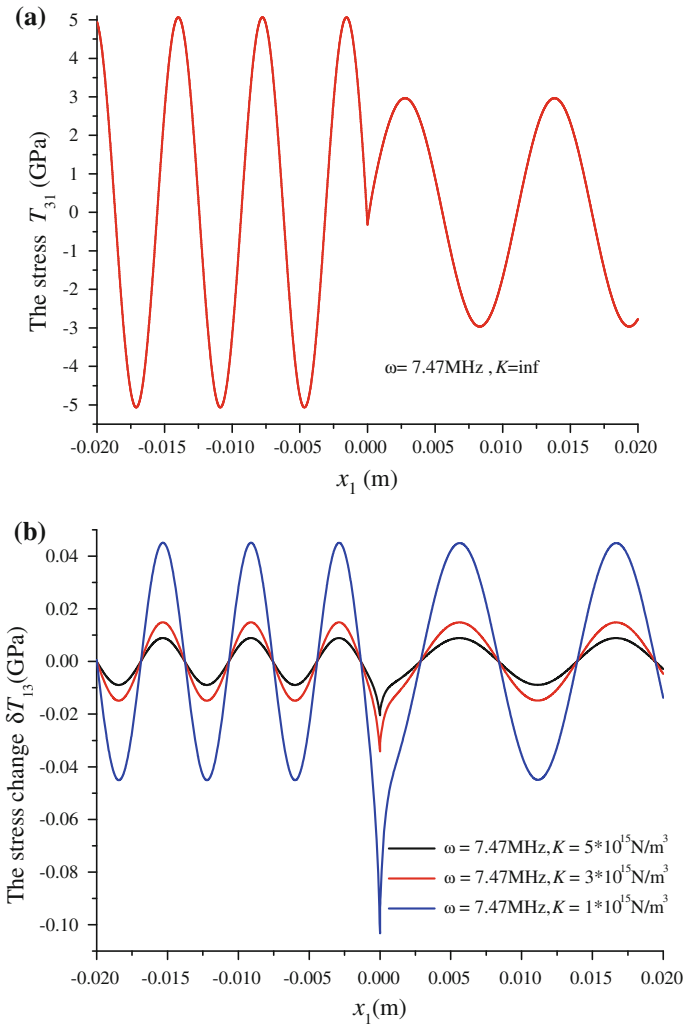

Fig. 8 The stress T_{13} and the stress change δT_{13} when $\omega = 7.47\,\mathrm{MHz}$. **a** The stress T_{13}, **b** the stress change δT_{13}

4 Conclusions

In order to depict the effect of the imperfect interface on the thickness-twist waves in an inhomogeneous piezoelectric plate, an exact solution is obtained by using the spring-type relation. Theoretical analysis and numerical simulation simultaneously show that the effect of mechanical imperfection is more evident than that of the electrical imperfection on the wave properties. It is shown that there will be zero-reflection waves when the frequency of the incident wave and the mechanical imperfection satisfy a particular relation. The results reported in this paper not only can be used as benchmark for the further investigation of wave propagation in the piezoelectric coupled structures, but also theoretically meaningful in the design of plate resonator and acoustic wave sensors with high performance.

Acknowledgments The financial support of the work by the National Natural Science Foundation of China (No. 10972171), the Specialized Research Fund for the Doctoral Program of Higher Education of China (No. 20070698064), and the Program for New Century Excellent Talents in Universities (No. NCET-08-0429) is gratefully acknowledged.

References

1. Karl, F.G.: Wave Motion in Elastic Solids. Clarendon Press, Oxford (1975)
2. Vellekoop, M.J.: Acoustic wave sensors and their technology. Ultrasonics **36**, 7–14 (1998)
3. Mindlin, R.D.: Bechmann's number for harmonic overtones of thickness-twist vibrations of rotated Y-cut quartz plates. J. Acoust. Soc. Am. **41**, 969–973 (1967)
4. Pearman, G.T.: Thickness-twist vibrations in beveled AT-cut quartz plates. J. Acoust. Soc. Am. **45**, 928–934 (1968)
5. Bleustein, J.L.: Thickness-twist and face-shear vibrations of a contoured crystal plate. Int. J. Solids Struct. **2**, 351–360 (1966)
6. Bleustein, J.L.: Some simple modes of wave propagation in an infinite piezoelectric plate. J. Acoust. Soc. Am. **45**, 614–620 (1969)
7. Yang, J., Chen, Z., Hu, Y.: Trapped thickness-twist modes in an inhomogeneous piezoelectric plate. Philos. Mag. Lett. **86**, 699–705 (2006)
8. Yang, J., Chen, Z., Hu, Y.: Propagation of thickness-twist waves through a joint between two semi-infinite piezoelectric plates. IEEE Trans. U F F C **54**, 888–891 (2007)
9. Yang, J.S., Chen, Z.G., Hu, Y.T., et al.: Propagation of thickness-twist waves in a multi-sectioned piezoelectric plate of 6 mm crystals. Arch. Appl. Mech. **77**, 689–696 (2007)
10. Qian, Z., Jin, F., Wang, Z., Kishimoto, K.: Transverse surface waves on a piezoelectric material carrying a functionally graded layer of finite thickness. Int. J. Eng. Sci. **45**, 455–466 (2007)
11. Qian, Z., Jin, F., Hirose, S., et al.: Effect of material gradient on transverse surface waves in piezoelectric coupled solid media. Appl. Phys. Lett. **95**, 073501–073503 (2009)
12. Nie, G., An, Z., Liu, J.: SH-guided waves in layered piezoelectric-piezomagnetic plates. Prog. Nat. Sci. **19**, 811–816 (2009)
13. Vig, J.R., Ballato, A.: Comments on the effects of nonuniform mass loading on a quartz crystal microbalance. IEEE Trans. U F F C **45**, 1123–1124 (1998)
14. Fan, H., Yang, J.S., Xu, L.: Piezoelectric waves near an imperfectly bonded interface between two half-spaces. Appl. Phys. Lett. **88**, 203509 (2006)
15. Jin, F., Kishimoto, K., Qing, H., et al.: Influence of imperfect interface on the propagation of Love waves in piezoelectric layered structures. Key Eng. Mater. **26**, 251–256 (2004)
16. Liu, H., Yang, J., Liu, K.: Love waves in layered graded composite structures with imperfectly bonded interface. Chin. J. Aeronaut. **20**, 210–214 (2007)
17. Huang, Y., Li, X.F., Lee, K.Y.: Interfacial shear horizontal (SH) waves propagating in a two-phase piezoelectric/piezomagnetic structure with an imperfect interface. Phil. Mag. Lett. **89**, 95–103 (2009)
18. Chen, J., Wang, W., Wang, J., et al.: A thickness mode acoustic wave sensor for measuring interface stiffness between two elastic materials. IEEE Trans. U F F C **55**, 1678–1681 (2008)
19. Li, Y.-D., Lee, K.Y.: Effect of an imperfect interface on the SH wave propagating in a cylindrical piezoelectric sensor. Ultrasonics **50**, 473–478 (2010)
20. Achenbach, J.D.: Wave Propagation in Elastic Solids. Northwestern University, Evanston (1973)
21. Peng, F., Hu, S.Y.: Investigation of shear horizontal acoustic waves in an inhomogeneous magnetoelectroelastic plate. Key Eng. Mater. **306–308**, 1217–1222 (2006)
22. Jiang, S.N., Jiang, Q., Li, X.F., et al.: Piezoelectromagnetic waves in a ceramic plate between two ceramic half-spaces. Int. J. Solids Struct. **43**, 5799–5810 (2006)